

A NONDIMENSIONAL ANALYSIS OF DUSTY SHOCK WAVES IN STEADY FLOWS

G. Ben-Dor*, M. Mond*, O. Igra* and Y. Martsiano*

(Received February 10, 1988)

The governing equations describing the flow field which results when a dust-gas suspension passes through a normal shock wave were nondimensionalized. The nondimensionalization resulted in a set of nondimensional groups of parameters which, if kept constant, lead to a self-similar solution. An investigation of these nondimensional groups of parameters revealed, for example, that the relaxation length depends linearly on the material density of the solid particles. Dependence of the relaxation length on the other parameters of the dust is discussed.

Key Words : Dusty Shock Waves, Gas-Solid Suspensions, Two-Phase Flows

1. INTRODUCTION

The interest in the gas-dynamic behaviour of a gas-particle suspension grew in the past three decades due to its application in many engineering problems. Some typical examples are: metalized propellents of rockets, jet-type dust collectors and blast waves in dusty atmospheres. In addition, mixtures with gases heavily laden with solid particles occur frequently in industrial processes such as plastics manufacturing, flour milling, coal-dust conveying, powder metalurgy and powdered-food processing. General descriptions of such flows can be found in several books and review papers [Soo (1967), Marble (1970) and Rudinger (1973)].

The major differences between the flow fields which are developed behind a normal shock wave in a dusty-gas and a pure (dust-free) gas are illustrated in Figs. 1a and b for the temperatures and the velocities, respectively. When a steady pure gas encounters a normal shock wave it experiences a sharp (almost discontinuous) change in its thermodynamic and kinematic properties. This sudden change is shown in Fig. 1 to occur between (0) and (1). The thickness of this disturbance, l_f , is only a few mean free paths of the gas atoms or molecules. Beyond (1) the gas properties remain constant (solid lines in Figs. 1a and b) provided the gas conditions at (1) are not sufficient to excite the internal degrees of freedom of the gas.

If, however, the gas is laden with solid particles then the suspension which was originally at a state of thermodynamic and kinematic equilibrium, ahead of the shock front, is suddenly changed into a non-equilibrium state, because the solid particles, due to their size compared with l_f , do not experience any noticeable change in their properties upon moving from (0) to (1). Thus, at (1) the gas has a much higher temperature than the dust, $T_g \gg T_p$ and a much lower velocity $u \ll v$.

Morgenthaler (1962) indicated that this is true even if the particle diameter is as small as $0.1 \mu\text{m}$ (for shock waves in air at nearly standard conditions, where the mean free path is about $0.066 \mu\text{m}$). Therefore, the particles are not influenced by the initial disturbance, and the gas properties at (1) can be safely assumed to be identical to those of a pure gas with the same initial conditions.

Far downstream of (1), i.e., at (∞) in Fig. (1), the gas and the

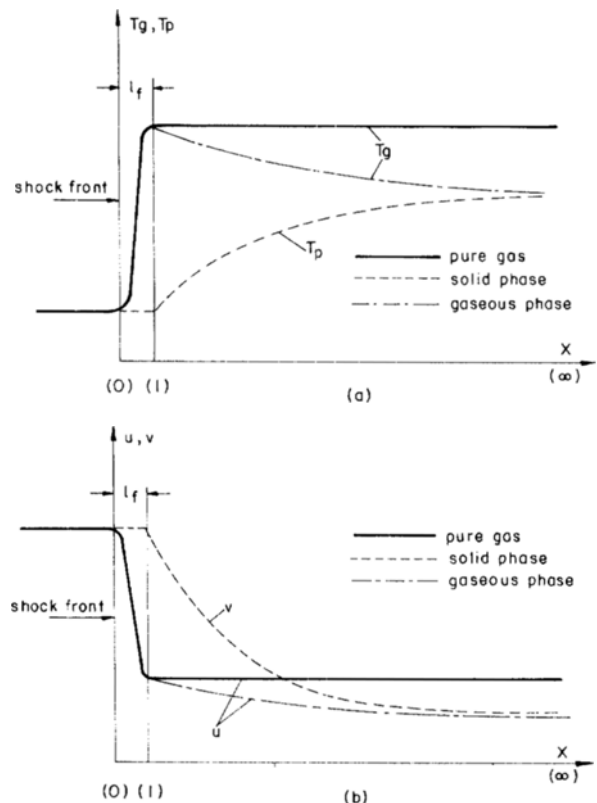


Fig. 1 A schematical illustration of the (a) temperatures and (b)

*The Pearlstone Center for Aeronautical Engineering Studies, Department of Mechanical Engineering, Ben-Gurion University of the Negev Beer Sheva, 84 105(P.O.B 653), Israel

solid phases reach a new state of thermodynamic and kinematic equilibrium via momentum and energy exchange. Theoretically all shock waves in dusty gases are infinitely thick, since equilibrium is approached asymptotically. However, it is a common practice to assign to the shock wave an effective thickness which is defined by a requirement that the suspension properties come close to their asymptotic downstream values. It was shown by Gottlieb and Coskunes (1985) that the suspension equilibrium properties (at infinity) can be calculated from the usual normal shock wave relations, provided that the usual pure gas parameters γ and R (the heat capacities ratio and the gas constant) are replaced by effective values $\bar{\gamma}$ and \bar{R} which solely depend on the initial conditions of the suspension.

Between (1) and (∞) the solid particles are not in equilibrium with the gas. The flow region between (1) and (∞) is known as the relaxation zone, for it is analogous to the relaxation zone in pure gases where the internal degrees of freedom are excited. The extent of the relaxation zone strongly depends on the momentum and heat transfer mechanisms which enable the solid and the gaseous phases to reach a new equilibrium state. The analysis of the relaxation zone was studied by many investigators. The pioneering works of Carrier (1958), Kriebel (1964) and Rudinger (1964) verified the existence of this relaxation zone and identified the parameters affecting it, namely; the solid particle diameter, D , its heat capacity, C , its material density, σ , and the loading ratio, η . Igra and Ben-Dor (1980) compared various correlations for the drag coefficient, C_D , and the heat transfer coefficient, Nu , and pointed out their effect on the extent of the relaxation zone. In addition they studied the role of thermal radiation heat transfer between the two phases and showed that it can be neglected when the incident shock waves Mach number is smaller than five.

In the present study a more general approach of investigating the dependence of the post shock flow field on the various physical parameters of the solid phase is presented. It is based on nondimensionalizing the governing equations and thereby obtaining a set of nondimensional groups of parameters, which if kept constant ensure a self-similar solution of the governing equations.

In the following, the basic assumptions upon which the present model is based are given. The assumptions are followed by the governing equations and the numerical results arising from their solution.

2. THEORETICAL BACKGROUND

2.1 Assumptions

The assumptions upon which the present model is based and their implications are listed in the following:

- (1) The gaseous phase behaves as an ideal gas. Thus, the equation of state of the gas is $P = \rho_g R T_g$. It is further assumed that the gas is calorically perfect, i.e., both C_p and C_v are assumed to be constant.
- (2) All solid particles are rigid, inert small spheres uniformly distributed in the gaseous phase. Thus there is no heat addition or reduction due to chemical processes between the solid and the gaseous phases. Furthermore, Re and Nu are based on the particle diameter, D .
- (3) The volume of the solid phase in the suspension can be neglected. Thus the momentum and energy exchange between the solid particles can be ignored.

(4) Aside from momentum and energy interactions between the gaseous and the solid phases, the gaseous phase is considered to be a perfect flow, i.e., its dynamic viscosity, μ_g , and its thermal conductivity, k_g , are zero. This also implies that neither kinematic nor thermal boundary layers develop around the solid particles.

(5) The solid particles are too large to experience any change in their thermodynamic and dynamic properties upon their passage through the shock front. In addition they are also large enough not to experience Brownian motion. Thus, the partial pressure of the solid phases can be neglected.

(6) The solid particles are such that they satisfy the condition $B_1 < 0.1$, where B_1 is the Biot number, $B_1 = hr/k_p$ (h is the coefficient of heat transfer, r is the radius of the particle, and k_p is its thermal conductivity). Thus the temperature within the solid particles can be assumed to be uniform.

(7) The weight of the solid particles and the buoyancy forces experienced by them are negligibly small in comparison with the drag forces acting on them.

(8) The heat capacity, C , of the solid particles is constant.

(9) Ahead of the normal shock wave the suspension is at a state of thermodynamic and kinematic equilibrium, i.e., $u_0 = v_0$ and $T_{g_0} = T_{p_0}$, where u and v are the velocities of the gas and the solid particles, and T_g and T_p are the temperatures of the gas and solid particles, respectively.

In addition to the above listed assumptions it is assumed that the flow under consideration is one-dimensional and steady.

2.2 Governing Equations

The development of the governing equations can be found in many papers and hence in the following only their final form is listed.

-continuity of the gaseous phase

$$\frac{d}{dx}(\rho_g u) = 0 \quad (1)$$

-continuity of the solid phase

$$\frac{d}{dx}(\rho_p v) = 0 \quad (2)$$

-conservation of linear momentum of the gaseous phase

$$\frac{d}{dx}(\rho_g u^{2+p}) = F_D \quad (3)$$

-conservation of linear momentum of the solid phase

$$\frac{d}{dx}(\rho_p v^2) = -F_D \quad (4)$$

-conservation of energy of the gaseous phase

$$\frac{d}{dx} \left[\rho_g u \left(C_p T_g + \frac{1}{2} u^2 \right) \right] = Q_{H.T.} + F_D v \quad (5)$$

-conservation of energy of the solid phase

$$\frac{d}{dx} \left[\rho_p v \left(C T_p + \frac{1}{2} v^2 \right) \right] = -Q_{H.T.} - F_D v \quad (6)$$

-equation of state of the gaseous phase

$$P = \rho_g R T_g \quad (7)$$

In the above equations ρ_g , u , T_g and P are the density, velocity, temperature and pressure of the gaseous phase, respectively. ρ_p , v and T_p are the spacial density, velocity and temperature of the solid phase respectively. Note that according to assumption 5 the partial pressure of the solid phase is zero. For this reason P is not only the pressure of the gaseous phase, but the pressure of the suspension as well. C_p and R are the specific heat capacity at constant pressure and the specific gas constant of the gaseous phase and C is the specific heat capacity of the particles of the particles of the solid phase. F_D is the drag force per unit volume exerted by the gaseous phase on the particles of the solid phase and $Q_{H.T.}$ is the heat transferred per unit volume from the solid phase to the gaseous phase.

The drag force, F_D , can be calculated from

$$F_D = \frac{3}{4} \rho_g \rho_p (v - u) |v - u| C_D / (D\sigma) \quad (8)$$

where D is the diameter of the solid particles, σ is their material density and C_D the drag coefficient is usually given by a function of the form

$$C_D = C_D(Re) \quad (9)$$

Since the Re number (see definition in Eq. 10) is very high immediately behind the shock front while its magnitude vanishes towards the end of the relaxation zone, where $v \approx u$ is approached, two different correlations were used for C_D . For $Re < 800$

$$C_D = \frac{24}{Re} (1 + 0.05 Re^{0.687})$$

and for $800 < Re < 3 \times 10^5$

$$C_D = \frac{24}{Re} (1 + 0.15 Re^{0.687}) + \frac{0.42}{1 + 42500 Re^{-1.16}}$$

The Reynolds number in the above expression is

$$Re = \frac{\rho_g |v - u| D}{\mu_g} \quad (10)$$

where μ_g is the dynamic viscosity of the gaseous phase.

The heat transferred from the gaseous phase to the solid phase can be calculated from

$$Q_{H.T.} = 6h\rho_p(T_p - T_g) / (D\sigma) \quad (11)$$

where h the coefficient of heat transfer can be obtained from

$$h = \frac{k_q Nu}{D} \quad (12)$$

The Nusselt number, Nu , is usually given by a function of the form

$$Nu = 2 + 0.459 Pr^{1/3} Re^{0.55} \quad (13)$$

In the last expression Pr is the Prandtl number, i.e.,

$$Pr = \frac{\mu_g C_p}{k_g} \quad (14)$$

where k_g (also in Eq. 12) is the thermal conductivity of the gaseous phase.

In summary the governing equations consist of 7 equations (four for the gaseous phase, i.e., conservation of mass, momentum and energy and the equation of state and three for the solid phases, i.e., conservation of mass, momentum and energy). The number of the unknowns in the above set of equations is also 7 (ρ_g , u , T_g and P for the gaseous phase and ρ_p , v and T_p for the solid phases). Thus the above set of governing equations is solvable in principle.

2.3 Nondimensionalization of the Governing Equations

Prior to numerically solving the above listed governing equations, let us first nondimensionalize the dependent and independent variables using the following nondimensional definitions.

$$u = \frac{u}{a_0}, \quad v = \frac{v}{a_0}, \quad x' = x \frac{x}{L}$$

$$\rho'_g = \frac{\rho_g}{\rho_{g_0}}, \quad \rho'_p = \frac{\rho_p}{\rho_{p_0}},$$

$$P' = \frac{P}{\rho_{g_0} a_0^2}, \quad T'_g = \frac{C_p T_g}{a_0^2}, \quad T'_p = \frac{C_p T_p}{a_0^2}$$

In the above definitions ρ_{g_0} is the density of the gaseous phase ahead of the shock wave, a_0 is the local speed of sound ahead of the shock wave and L is the relaxation length. Inserting the above definitions into the above listed governing equations, results in the following set of nondimensional equations (note that for simplicity the prime sign is omitted, but from this stage on, all the independent and dependent variables are nondimensional).

-nondimensional conservation of the mass of the gaseous phase

$$\frac{d}{dx}(\rho_g u) = 0 \quad (15)$$

-Nondimensional conservation of the mass of the solid phase

$$\frac{d}{dx}(\rho_p v) = 0 \quad (16)$$

-Nondimensional conservation of the linear momentum of the gaseous phase

$$\frac{d}{dx}(\rho_g u^{2+p}) = \frac{3}{4} \frac{\rho_{g_0}}{\sigma} \frac{L}{D} \rho_g \rho_p (v - u) |v - u| C_D \quad (17)$$

-Nondimensional conservation of the linear momentum of the solid phase

$$\frac{d}{dx}(\rho_p v^2) = -\frac{3}{4} \frac{\rho_{g_0}}{\sigma} \frac{L}{D} \rho_g \rho_p (v - u) |v - u| C_D \quad (18)$$

-Nondimensional conservation of the energy of the gaseous phase

$$\frac{d}{dx} \left[\rho_g u \left(T_g + \frac{1}{2} u^2 \right) \right] = 6 \frac{\rho_{g_0}}{\sigma} \frac{L}{D} \frac{Nu}{Re Pr} \rho_g (T_p - T_g) + \frac{3}{4} \frac{\rho_{g_0}}{\sigma} \frac{L}{D} (v - u) |v - u| v C_D \quad (19)$$

-Nondimensional conservation of the energy of the solid phase

$$\frac{d}{dx} \left[\rho_p v \left(\delta T_p + \frac{1}{2} v^2 \right) \right] = -6 \frac{\rho_{g0}}{\sigma} \frac{L}{D} \frac{Nu}{R\mathfrak{E}Pr} \rho_g (T_p - T_g) - \frac{3}{4} \frac{\rho_{g0}}{\sigma} \frac{L}{D} (v-u) |v-u| \nu C_D \quad (20)$$

-The nondimensional equation of state of the gaseous phase

$$P = \frac{R}{C_p} \rho_g T_g = \frac{\gamma-1}{\gamma} \rho_g T_g \quad (21)$$

In the above set of nondimensional equations

$$R\mathfrak{E} = \frac{\rho_{g0} a_0 D}{\mu_g}, \quad \delta = \frac{C}{C_p} \text{ and } \gamma = \frac{C_p}{C_v}$$

The above set of nondimensional governing equations implies that if $R\mathfrak{E}$, Nu , Pr , δ , γ and $\frac{\rho_{g0}}{\sigma} \frac{L}{D}$ are kept constant, then the solution of the governing equations is self-similar. While the first five nondimensional groups are well known, the sixth one has never been mentioned in the past, in any of the known published papers. Physically it is a measure of the coupling between the gaseous and the solid phases.

2.4 Numerical Verification and Discussion

The solution of the dimensional governing equations, i.e., equations 1 to 7 is shown in Fig. 2 for three different cases.

For all the three cases, the incident shock wave Mach number is $M_0=2$, the loading ratio of the dust phase in the

suspension is $\eta=0.1$, the diameter of the solid particles is $D=100\mu\text{m}$ and their specific heat capacity is $C=1000\text{J}/(\text{Kg K})$. The three cases differ in their material density- σ . In Fig. 2a $\sigma=1000\text{Kg}/\text{m}^3$, in Fig. 2b $\sigma=2500\text{Kg}/\text{m}^3$ and in Fig. 2c $\sigma=5000\text{Kg}/\text{m}^3$.

The flow fields which result for these three cases are plotted in Figs. 2a, b and c, in which the horizontal scale is 4, 10 and 20 m. Note that the horizontal scales are proportional to the material densities, i.e., 1000 : 2500 : 5000 and 4 : 10 : 20.

In view of the above discovery of the existence of the following nondimensional group $\frac{\rho_{g0}}{\sigma} \frac{L}{D}$ it is not surprising that the various property profiles of the flow fields shown in Figs. 2a, b and c, are identical. This is due to the fact that the material density σ affects only this nondimensional group out of the six mentioned earlier. Thus, by scaling down the horizontal axis of Figs. 2b and c proportionally to the increase in the material density, σ , the value of the nondimensional group $\frac{\rho_{g0}}{\sigma} \frac{L}{D}$ was also kept constant (in addition to the other five nondimensional groups which, as mentioned earlier, are unaffected by the material density of the solid particles). This, in turn, resulted in a self-similar solution as shown in Fig. 2.

The foregoing discussion can be summarized by the following conclusion : The relaxation length, L , depends linearly on the material density of the solid particles, σ , i.e.

$$\frac{\sigma_1}{\sigma_2} = \frac{L_1}{L_2}$$

Inspection of the six nondimensional groups, i.e.,

$$R\mathfrak{E} = \frac{\rho_{g0} a_0 D}{\mu_g}, \quad Pr = \frac{\mu_g C_p}{k_g}, \quad Nu = \frac{hD}{k_g},$$

$$\delta = \frac{C}{C_p}, \quad \gamma = \frac{C_p}{C_v} \text{ and } \frac{\rho_{g0}}{\sigma} \frac{L}{D}$$

indicates that the dependence of the relaxation length, L , on the remaining two physical properties of the dust particles, namely their diameter, D , and specific heat capacity, C , is not as simple as its above mentioned dependence on the material density. For example a change in the diameter of the solid particles, D , influences three of the six nondimensional groups. However, as an exercise, the following problem was solved numerically $M_0=2$, $\eta=0.1$, $C=1000\text{J}/(\text{Kg K})$, $\sigma=1000\text{Kg}/\text{m}^3$ and $D=200\mu\text{m}$. This diameter is twice as big as that used in Fig. 2a. In addition to the change in the diameter of the solid particles, the dynamic viscosity and thermal conductivity of the gaseous phase were set, artificially, to be equal to twice their respective values in the case shown in Fig. 2a. If the properties of the case shown in Fig. 2a, which were changed in the considered artificial case, are denoted by a subscript "r", then the values of the six nondimensional groups for this artificial case become :

$$R\mathfrak{E} = \frac{\rho_{g0} a_0 2D_r}{2\mu_{gr}} = \frac{\rho_{g0} a_0 D_r}{\mu_{gr}}$$

$$Pr = \frac{2\mu_{gr} C_p}{2k_{gr}} = \frac{\mu_{gr} C_p}{k_{gr}}$$

$$Nu = \frac{h2D_r}{2k_{gr}} = \frac{hD_r}{k_{gr}}$$

$$\delta = \frac{C}{C_p}, \quad \gamma = \frac{C_p}{C_v} \text{ and}$$

$$\frac{\rho_{g0} L}{\sigma 2D_r} = \frac{\rho_{g0} (0.5L)}{\sigma D_r}$$

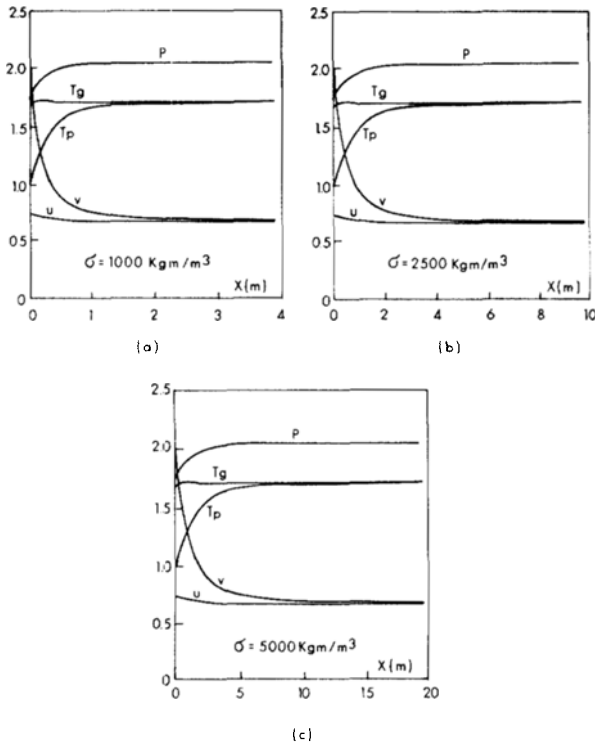


Fig. 2 The profiles of the various suspension properties in the relaxation zone for: $M_0=2$, $\eta=0.1$, $D=100\mu\text{m}$, $C=1000\text{J}/(\text{Kg K})$ and different values of σ which appear in the figures

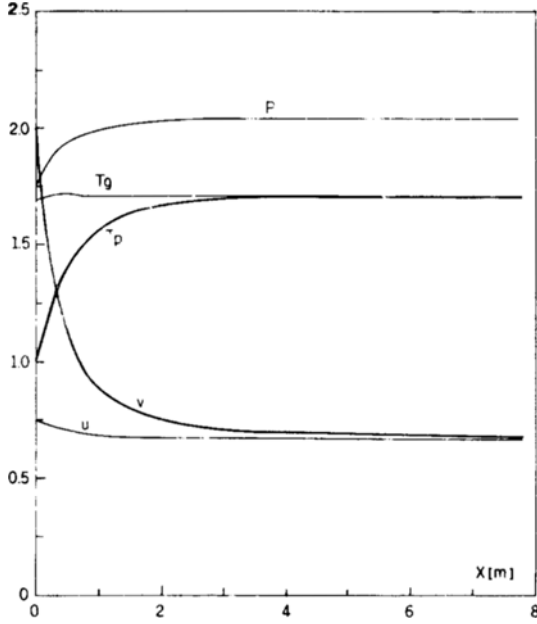


Fig. 3 The profiles of the various suspension properties in the relaxation zone for: $M_o=2$, $\eta=0.1$, $D=200\mu\text{m}$, $C=1000\text{J}/(\text{Kg K})$, $\mu_g=2\mu_{g2}$ and $k_g=2k_{g2}$, where μ_{g2} and k_{g2} are the dynamic viscosity and thermal conductivity of the three cases shown in Fig. 2

Thus, it is evident that if the horizontal scale is scaled down by a factor of two, then the values of the six nondimensional groups of the artificial case become identical to those of the reference case denoted by "r" and, hence, the numerical solution of the artificial case should be self-similar to the reference case. Fig. 3, which represents the numerical solution of the artificial case, indeed verifies that the solution of the artificial case is identical to that of the reference case.

2.5 The Dependence of the Loading Ratio

Although the above nondimensional analysis resulted in six nondimensional groups, namely: Re , Pr , Nu , δ , γ and $\frac{\rho_{g0}}{\sigma} \frac{L}{D}$, there is another very important nondimensional parameter, which has a significant effect on the post shock flow field. It is the dust loading ratio, η . The value of η determines the intensity of the coupling between the two phases. This can be shown by using the conservation equations of the two phases. Integrating equations (1) and (2) results in:

$$\rho_g u = \rho_{g0} u_0 \quad (22a)$$

and

$$\rho_p v = \rho_{p0} v_0 \quad (22b)$$

Dividing these two equations yields:

$$\frac{\rho_p v}{\rho_g u} = \frac{\rho_{p0} v_0}{\rho_{g0} u_0}$$

But using the condition that ahead of the shock wave, in state (0), the suspension is in a kinematic equilibrium, i.e., $u_0 = v_0$ the above expression becomes:

$$\frac{\rho_p v}{\rho_g u} = \frac{\rho_{p0}}{\rho_{g0}} = \eta \quad (23)$$

where η is the dust loading ratio.

Equation (23) implies that the loading ratio, η , determines the ratio between the rate of flow of the dusty phase and that of the gaseous phase. The higher η is, the greater the amount of the dust in the suspension.

It should be noted that there are publications where the loading ratio is defined in a different way:

$$\eta^* = \frac{\rho_{p0}}{\rho_{p0} + \rho_{g0}} \quad (24)$$

Thus while it is clear from Eq. (23) that $0 < \eta < \infty$, Eq. (24) implies that $0 < \eta^* < 1$. Note that in both cases the upper limit of the loading ratio (η or η^*) is only mathematical, since assumption 3 puts a physical upper limit on the loading ratio. This physical upper limit can be calculated in the following way:

The volume occupied by the solid particles, V_p , is:

$$V_p = \frac{m_p}{\sigma} N$$

where m_p is the mass of a single solid particle, σ is its material density and N is the number of solid particles in a given volume of suspension v . On the other hand $m_p N = M_p$ where M_p is the mass of all the solid particles in the given volume V . Dividing both sides of the above expression by V results in

$$\frac{V_p}{V} = \frac{\rho_{p0}}{\sigma}$$

where ρ_{p0} is the spatial density of the solid particles ahead of the shock wave. If 1% limit on the volume of the solid particles is assumed to satisfy the limit imposed by assumption 3 then:

$$\eta = \frac{\rho_{p0}}{\rho_{g0}} \leq 0.01 \frac{\sigma}{\rho_{g0}} \quad (25)$$

For a typical dust with material density $\sigma = 2000 \text{ Kg/m}^3$ in air at atmospheric conditions $\rho_{g0} \approx 0.8 \text{ Kg/m}^3$ Eq. (25) results in

$$\eta \leq 25. \quad (25a)$$

Finally it is of interest to note that the above mentioned two different definitions for the loading ratio are simply related by

$$\eta^* = \frac{\eta}{1 + \eta} \quad (26)$$

Thus the limit on η (Eq. 25a) implies that

$$\eta^* \leq 0.96 \quad (26a)$$

As discussed in Igra and Ben-Dor (1988), the dust-gas suspension ahead of the shock wave can be considered as a pseudo single phase gas having the following specific heat capacities:

$$\begin{aligned} \bar{C}_p &= \eta^* C + (1 - \eta^*) C_p \\ \bar{C}_v &= \eta^* C + (1 - \eta^*) C_v \end{aligned}$$

These specific heat capacities, result in:

$$\bar{\gamma} = \frac{\bar{C}_p}{\bar{C}_v} = \frac{\eta^* C + (1-\eta^*) C_p}{\eta^* C + (1-\eta^*) C_v}$$

which can be rewritten in the following way :

$$\bar{\gamma} = \gamma \frac{\eta^* \delta + (1-\eta^*)}{\eta^* \gamma \delta + (1-\eta^*)} \quad (27)$$

where δ is one of the nondimensional parameters mentioned previously, i.e., $\delta = C/C_p$. In addition, the local speed of sound of this pseudo-simple phase gas is

$$\bar{a} = \bar{\gamma} \bar{R} T_g$$

where $\bar{R} = (1-\eta^*) R$. This speed of sound results in a new Mach number for the pseudo-single phase gas :

$$\bar{M}_o = \frac{u_o}{\bar{a}}$$

It can be also shown that $\bar{a} < a$ and hence $\bar{M}_o > M_o$. Using the Rankine-Hugoniot equation with \bar{M}_o and $\bar{\gamma}$ rather than M_o and γ results in the values of the suspension properties at the end of the relaxation zone. however, since both \bar{M}_o and $\bar{\gamma}$ depend on η^* it is clear that the suspension properties at the end of the relaxation zone also depend on η^* .

The strong dependence of the suspension properties on the loading ratio η is shown in Fig. 4, which is a reproduction (dashed lines) of the results shown in Fig. 2a, with the addition (solid lines) of the numerical solution for the conditions $M_o=2$, $D=100\mu\text{m}$, $C=1000\text{J}/(\text{Kg K})$, $\sigma=1000\text{Kg}/\text{m}^3$ and $\eta=1$. Note that the only difference between the two cases is in η which is changed from 0.1 to 1. The change in the suspension properties at the end of the relaxation is clearly evident.

In order to illustrate again the self similarity of the solution, the case shown in Fig. 4 is replotted in Fig. 5a in a slightly different horizontal scale. A similar calculation but

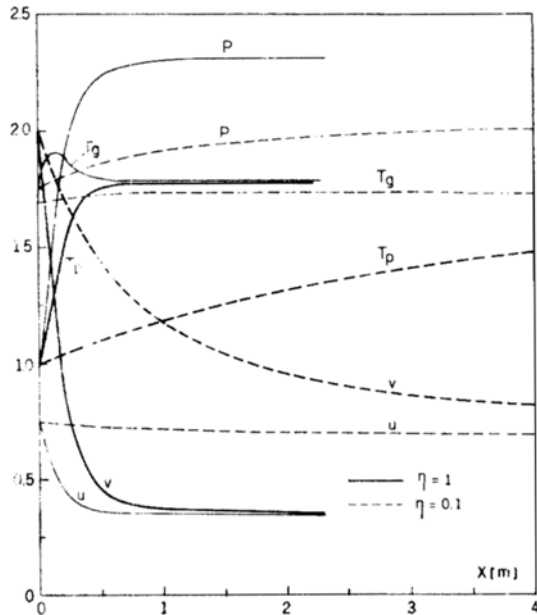


Fig. 4 The profiles of the various suspension properties in the relaxation zone for : $M_o=2$, $D=100\mu\text{m}$, $C=1000\text{J}/(\text{Kg K})$, $\sigma=1000\text{Kg}/\text{m}^3$ and different values of η which appear in the figures.

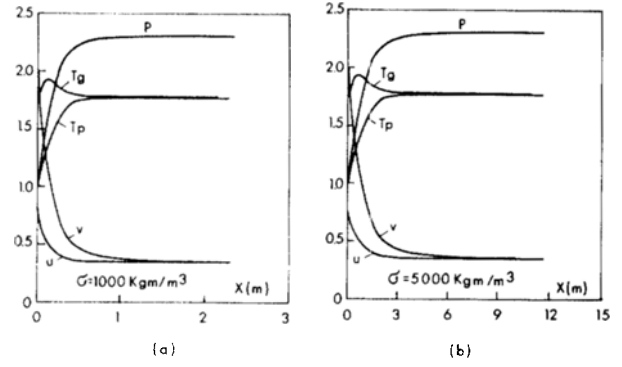


Fig. 5 The profiles of the various suspension properties in the relaxation zone for : $M_o=2$, $\eta=1$, $D=100\mu\text{m}$, $C=1000\text{J}/(\text{Kg K})$ and different values of σ which appear in the figures

for $\sigma=5000\text{Kg}/\text{m}^3$ rather than $1000\text{Kg}/\text{m}^3$ is shown in Fig. 5b. Since the material density is increased by a factor of five, the scale in Fig. 5b is extended by a factor of five. The profile shapes in Figs. 5a and 5b are identical.

3. CONCLUSIONS

A nondimensional analysis of dusty shock waves resulted in seven nondimensional groups of parameters which, if maintained constant, yield a self-similar solution. The seven nondimensional groups and parameters are :

$$R\bar{b} = \frac{\rho_{go} a_o D}{\mu_g}, \quad Pr = \frac{\mu_g C_p}{k_g}, \quad Nu = \frac{hD}{k_g}$$

$$\delta = \frac{C}{C_p}, \quad \gamma = \frac{C_p}{C_v}, \quad \eta = \frac{\rho_{po}}{\rho_{go}} \text{ and } \frac{\rho_{go} L}{\sigma D}$$

From the last nondimensional group which to the best of our knowledge has not been mentioned in the past, it is evident that relaxation length, L , depends linearly on the material density of the solid particles, σ , i.e.,

$$\frac{L_1}{L_2} = \frac{\sigma_1}{\sigma_2}$$

provided that the particle diameter and the initial conditions of the gaseous phase are kept constant.

REFERENCES

Carrier, G.F., 1958, "Shock Waves in a Dusty Gas", Journal Fluid Mechanics, Vol. 4, pp. 376~382.
 Gottlieb, J.J. and Coskunes, C.E., 1985, "Effects of particle Volume on a Partly Dispersed Normal Shock Wave in a Dusty Gas", UTIAS Report No. 295.
 Igra, O. and Ben-Dor, G., 1980, "Parameters Affecting the Relaxation Zone Behind Normal Shock Waves in Dusty Gases", Israel Journal of Technology, Vol. 18, pp. 159~168.
 Igra, O. and Ben-Dor, G., 1988, "Shock Waves in Dusty Gases", Applied Mechanics Review, to be published.
 Kriebel, A.R., 1964, "Analysis of Normal Shock Waves in a Particle Laden Gas", Journal Basic Engineering, Transactions ASME, Ser D86, 655~663.
 Marble, F.E., 1970, "Dynamics of Dusty Gases", Annual

Review Fluid Mechanics, Vol. 2, pp. 397~446.

Morgenthaler, J.H., 1962, "Analysis of Two Phase Flow in Supersonic Exhausts", Progress in Astronautics & Aeronautics, Vol. 6, pp. 145~171.

Rudinger, G., 1964, "Some Properties of Shock Relaxation in a Gas Flow Carrying Small particles", Physics Fluids, Vol.

7, pp. 658~663.

Rudinger, G., 1973, "Wave Propagation in Suspension of Solid Particles in Gas Flow", Applied Mechanics Review, Vol. 26, pp. 273~279.

Soo, S.L., 1967, "Fluid Dynamics of Multiphase Systems", Blaisdell Publishing Co., Waltham, Mass.